forests

MDPI

Article

Aboveground Wood Production Is Sustained in the First Growing Season after Phloem-Disrupting Disturbance

Maxim S. Grigri [1], Jeff W. Atkins [1], Christoph Vogel [2], Ben Bond-Lamberty [3] and Christopher M. Gough [1,*]

1 Department of Biology, Virginia Commonwealth University, Richmond, VA 23059, USA; grigrims@mymail.vcu.edu (M.S.G.); jwatkins6@vcu.edu (J.W.A.)
2 Biological Station, University of Michigan, Pellston, MI 49769, USA; csvogel@umich.edu
3 Pacific Northwest National Laboratory, Joint Global Change Research Institute, 5825 University Research Ct, College Park, MD 20740, USA; bondlamberty@pnnl.gov
* Correspondence: cmgough@vcu.edu

Received: 1 October 2020; Accepted: 4 December 2020; Published: 5 December 2020

Abstract: Carbon (C) cycling processes are particularly dynamic following disturbance, with initial responses often indicative of longer-term change. In northern Michigan, USA, we initiated the Forest Resilience Threshold Experiment (FoRTE) to identify the processes that sustain or lead to the decline of C cycling rates across multiple levels (0, 45, 65 and 85% targeted gross leaf area index loss) of disturbance severity and, in response, to separate disturbance types preferentially targeting large or small diameter trees. Simulating the effects of boring insects, we stem girdled > 3600 trees below diameter at breast height (DBH), immediately and permanently disrupting the phloem. Weekly DBH measurements of girdled and otherwise healthy trees ($n > 700$) revealed small but significant increases in daily aboveground wood net primary production ($ANPP_w$) in the 65 and 85% disturbance severity treatments that emerged six weeks after girdling. However, we observed minimal change in end-of-season leaf area index and no significant differences in annual $ANPP_w$ among disturbance severities or between disturbance types, suggesting continued C fixation by girdled trees sustained stand-scale wood production in the first growing season after disturbance. We hypothesized higher disturbance severities would favor the growth of early successional species but observed no significant difference between early and middle to late successional species' contributions to $ANPP_w$ across the disturbance severity gradient. We conclude that $ANPP_w$ stability immediately following phloem disruption is dependent on the continued, but inevitably temporary, growth of phloem-disrupted trees. Our findings provide insight into the tree-to-ecosystem mechanisms supporting stand-scale wood production stability in the first growing season following a phloem-disrupting disturbance.

Keywords: disturbance; aboveground net primary production; carbon cycle; eastern forests; disturbance severity; disturbance type; compensatory growth; successional cohort; leaf area index

1. Introduction

The spatial footprint of disturbance from wood boring insect pests is immense, but the resulting effects of phloem disruption on carbon (C) storage in wood remains uncertain [1]. Each year in the United States alone, an estimated 2.4 Mha of forestland is invaded by phloem-disrupting insects [2], giving rise to large gradients of stand-scale disturbance severity [1,3–5]. While C cycling responses to stand-replacing disturbance are well-studied, the mechanisms underlying whole ecosystem C cycling responses to less severe phloem-disrupting disturbances are poorly understood [2,5–9]. Notably, phloem disruption may result in a more gradual reduction in tree growth relative to disturbances from fire, extreme

weather and partial harvesting [10,11]. However, whether the collective growth of phloem-disrupted trees sufficiently sustains stand-scale production in the near-term cannot be determined from current knowledge, which is derived from the tree-scale analyses of a limited number of species.

While untested empirically, tree physiology and modeling studies suggest a sequence of changes combine to initially stabilize stand-level production following phloem disrupting disturbance. First, tree-scale studies consistently show that stem girdling, a process physiologically similar to the effects of wood boring pests, eliminates the transport of newly fixed C to the roots, resulting in an accumulation of C in the stem and shoots [12–15]. Changes in C allocation after girdling may thus reduce belowground growth and temporarily increase aboveground production [16,17]. The duration and extent of aboveground growth following girdling varies substantially among species, study systems and methodologies [13,16,18–23], however, suggesting that sustained stand-scale aboveground production from phloem-disrupted tree growth is not automatic and could be short-lived. Once phloem-disrupted tree growth declines, resource reallocation may stimulate the compensatory growth of healthy trees and stabilize stand-scale aboveground production [13,22–24]. The timing and magnitude of healthy-tree compensatory growth, along with its contribution to total aboveground production across a range of disturbance severities, is unknown but constitutes a potential mechanism underlying the stabilization of stand-scale production in the first year following phloem disruption [10,25–27]. Connecting tree-scale responses to whole-ecosystem wood production is critical to developing a comprehensive empirical understanding of the dynamic processes before, during, and after tree mortality, that regulate C cycling changes following disturbance.

We used a large-scale stem girdling manipulation to characterize the initial response of stand-scale aboveground wood net primary production ($ANPP_w$) to a range of disturbance severities (0, 45, 65 and 85% targeted gross leaf area index loss) and two disturbance types (top-down and bottom-up) affecting different stem size classes. Our goal is to provide an in-depth mechanistic look at what is hypothesized to be a highly dynamic period immediately following disturbance [27], by examining at a fine (i.e., weekly) time scale the plant-to-ecosystem sources of C cycling stability in the first year following disturbance. More broadly, we are motivated to understand, at the stand scale, the mechanisms that drive differences in initial C cycling responses to moderate severity disturbance [1,2,4,28,29], and build on other first year analyses of C cycling responses to the Forest Resilience Threshold Experiment (FoRTE) disturbance [30]. Our specific objectives were to examine daily and annual $ANPP_w$ at multiple disturbance severity levels and in two disturbance types; the contribution of girdled and healthy (i.e., not girdled) trees to $ANPP_w$; and early and middle to late successional tree species contributions to annual $ANPP_w$ as disturbance severity increases. We hypothesized that girdled trees would continue to grow at the same rate immediately after disturbance, but that their contribution to $ANPP_w$ would gradually decline in the first year and, consequently, the compensatory growth of healthy trees would increase over the course of the growing season. We anticipated that annual $ANPP_w$ would remain stable at or below a 65% disturbance severity threshold [31], while declining at the highest disturbance severity of 85%. Lastly, we predicted that early successional species, which may respond with greater vigor to newly liberated resources [32], would contribute more to $ANPP_w$ as disturbance severity increases.

2. Materials and Methods

2.1. Site Description

Our research took place at the University of Michigan Biological Station (UMBS) (45°35′ N 84°43′ W) in northern Michigan, USA. In 2019, the year of core data collection, mean annual temperature and precipitation were within the historical range for our site at 5.4 °C and 97.46 cm [33]. Like many present-day hardwood forests in the upper Midwest, the 100 year-old regrown forest is shifting from early successional aspen (*Populus* spp.) and birch (*Betula* spp.) to later successional northern red oak (*Quercus rubra*), red maple (*Acer rubrum*), and to a lesser extent, sugar maple (*A. saccharum*), American beech (*Fagus grandifolia*), white pine (*Pinus strobus*), and eastern hemlock (*Tsuga canadensis*) [34].

The subcanopy is primarily red maple and northern red oak, while American beech, sugar maple, serviceberry (*Amelanchier spp.*), white pine, red pine (*Pinus resinosa*), striped maple (*Acer pensylvanicum*) and balsam fir (*Abies balsamea*) are also present.

In May of 2019, we initiated the Forest Resilience Threshold Experiment (FoRTE) to examine C cycling responses to multiple disturbance severities and two disturbance types. The experiment used stem girdling (n > 3600 trees) to implement four replicated factorial combinations of disturbance severity at 0% (control), 45, 65 or 85% targeted gross leaf area index (LAI) loss, and a top-down or bottom-up disturbance type treatment meant to simulate structural changes in response to disturbances like beech bark disease or low severity subcanopy fire [6] that disproportionately impact large and small diameter trees, respectively. We acknowledge, however, that our experimental approach, intended to isolate the effects of disturbance severity and type, does not perfectly emulate the structural and compositional changes associated with natural disturbance. Canopy strata are defined as follows: upper canopy (≥8 cm diameter at breast height, DBH), subcanopy (1–8 cm DBH), and seedling/sapling (DBH < 1 cm or <1.3 m height). Prior to implementing the girdling disturbance, site or region-specific allometric equations relating DBH to leaf area were used to estimate the leaf area of each upper canopy tree within a plot [26,35]. Next, upper canopy stems were stem-girdled until the sum of affected tree leaf area reached the targeted gross LAI loss of each disturbance severity. For the bottom-up treatment, upper canopy stems with the smallest leaf areas were girdled first, irrespective of species. Conversely, the top-down treatment targeted larger stems, girdling trees with the highest leaf areas first until the disturbance severity was reached. For stem girdling, a 10 cm strip of bark was removed by chainsaw and pry bar at ~1 m height allowing for ~30 cm distance between the injured phloem tissue and breast height (~1.3 m height). Throughout the manuscript, we refer to stem-girdled trees as girdled and, for brevity, trees that were not experimentally girdled as healthy, while acknowledging the latter encompasses individuals spanning a range of physiological competencies and vigor.

Each replicated factorial combination of disturbance severity and type was contained within separate previously mapped experimental blocks varying in site productivity, soils, landform and species composition with either oak or aspen dominated canopies [36] (Table 1, Figure 1). Our replicated study design accounts for C cycling responses to disturbance treatments across an array of forest ecosystems present in the region. Upper canopy species composition for each treatment replicate was calculated as the percent of total biomass within subplots. Subcanopy and seedling/sapling composition was the relative stem density of each species within experimental subplots. Biomass was estimated using species, site and region-specific allometric equations relating diameter at breast height (DBH) to aboveground biomass [37] and scaled to the hectare (Table 1). Disturbance severity was randomly assigned to each of four, 0.5-ha whole-plots, which were bisected from north to south into split-plots and designated as top-down or bottom-up disturbance type treatments (Figure 1B). Circular 0.1-ha subplots with a treatment buffer of ~5 m surrounding the perimeter were established at the center of each split-plot for a total of 32 subplots, within which data collection for the derivation of $ANPP_w$ occurred (Figure 1).

Table 1. Predisturbance tree species composition and stem densities by canopy class, and total aboveground woody biomass for each of four treatment replicates (Figure 1). Canopy classes are defined by diameter at breast height (DBH). The four most abundant canopy and seedling/sapling species, and the five most abundant subcanopy species, are provided. Species abbreviations are: *Populus grandidentata* (POGR), *Quercus rubra* (QURU), *Acer rubrum* (ACRU), *Acer saccharum* (ACSA), *Fagus grandifolia* (FAGR), *Pinus strobus* (PIST), *Pinus resinosa* (PIRE), *Acer pensylvanicum* (ACPE), *Amelanchier* (AMEL), and *Viburnum acerifolium* (VBAC). Standard errors for stem densities and biomass are presented parenthetically.

	A	B	C	D
Upper canopy tree (≥8 cm DBH) biomass	POGR (61%) ACSA (17%) ACRU (10%) FAGR (10%)	POGR (58%) ACRU (24%) QURU (9%) FAGR (4%)	QURU (43%) POGR (39%) PIST (6%) ACRU (6%)	QURU (72%) POGR (19%) PIST (4%) FAGR (1%)
Subcanopy tree (1–8 cm DBH) relative density	FAGR (49%) ACPE (42%) ACSA (4%) ACRU (3%) AMEL (2%)	FAGR (42%) ACRU (24%) ACPE (13%) AMEL (11%) QURU (9.5%)	PIST (40%) ACRU (19%) FAGR (19%) ACPE (18%) QURU (2%)	PIST (53%) ACRU (33%) FAGR (8%) QURU (4%) PIRE (2.4%)
Seedling/sapling (<1 cm DBH) relative density	ACPE (35%) ACRU (34%) ACSA (19%) FAGR (7%)	ACRU (78%) AMEL (8%) VBAC (6%) ACPE (4%)	ACRU (66%) ACPE (13%) AMEL (11%) PIST (5%)	ACRU (71%) AMEL (16%) PIST (5%) QURU (4%)
Upper canopy stem density (stems ha^{-1}, ≥8 cm DBH)	865 (32)	888 (46)	910 (55)	796 (81)
Subcanopy stem density (stems ha^{-1}, 1–8 cm DBH)	2050 (356)	2630 (343)	1690 (331)	1045 (148)
Seedling/sapling stem density (stems ha^{-1}, <1 cm DBH)	208,125 (18,280)	243,871 (24,799)	53,125 (6513)	61,379 (9188)
Biomass (Kg C ha^{-1})	264,600 (15,800)	229,900 (24,700)	197,000 (13,900)	155,900 (19,000)

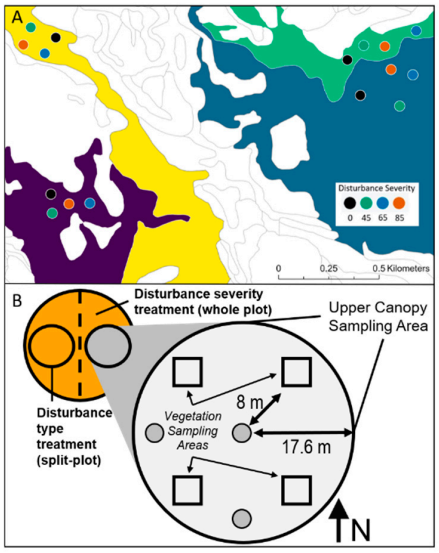

Figure 1. Disturbance treatment replicate distribution (**A**) and the split-plot experimental design (**B**) of the Forest Resilience Threshold Experiment (FoRTE) [30]. Treatment replicates serving as experimental blocks are distributed across four distinct forest ecosystems that are common to the region, and which are delineated above using the color scheme of Table 1. Lines distinguish between forest ecosystems varying by site productivity, soils, landform and species composition (**A**) [36]. Each replicate contains whole plots that were randomly assigned disturbance severities of 0, 45, 65 or 85% gross leaf area index loss and then split by top-down or bottom-up disturbance type (**B**).

2.2. Leaf Area Index

We estimated postdisturbance upper canopy leaf area index (LAI) from hemispherical images taken with a SONY Alpha 6000 24.3-megapixel DSLR camera with a 180-degree hemispherical lens. Images were taken 1 m above the forest floor at five nonoverlapping locations within each subplot beginning in May 2019 and continuing weekly through August 2019 [38] (FoRTE Project Data, https://fortexperiment.github.io/fortedata/). Images were processed for LAI using WinsCanopy (Regent Instruments, Quebec, Qu).

2.3. Aboveground Wood Net Primary Production

We derived daily and annual $ANPP_w$ for 2019 from repeated measurements of DBH (or, in the case of seedlings, basal diameter) [39]. During summer 2018, we censused upper canopy trees within each subplot, identifying individuals to the species level. In the same field season, we installed dendrometer bands at 1.3 m height on ~25% of all canopy trees (n = 666 total) using a stratified random selection process to ensure our banded subsample spanned the species abundances and DBH distributions of each subplot population. Dendrometer bands were custom made using $\frac{1}{2}$ inch steel tape, 2 inch stainless steel springs and circumference ruler stickers. Before installing dendrometer bands, a thin, outer layer of bark was mechanically shaved to achieve a smooth, tight fit around the stem. The DBH of banded trees was recorded during a one-year period on 17 separate one to two-day measurement campaigns on the following dates: November 2018; April 2019; weekly from May through August 2019 and November 2019.

Daily relative growth rates (RGRs, cm cm^{-1} day^{-1}) of banded trees were estimated as the diameter growth increment of a time interval divided by the diameter at the start of the time interval. When species and plot-specific linear relationships between DBH and RGR were significant ($p < 0.05$) in a time interval, we modeled the RGR of the unsampled tree populations using regression equations generated from observations. When relationships between DBH and RGR were not significant, we estimated RGRs of the unsampled population from week, subplot and species-specific mean RGRs. From measured or RGR-inferred DBH, we estimated aboveground wood biomass of upper canopy stems using species and site or region-specific allometries [34,37]. With the goal of understanding how tree-level responses to girdling scale to influence the stand-level $ANPP_w$, we separately compared the RGRs of girdled and healthy tree species using unpaired t-tests.

For subcanopy stems, we estimated density via species-level censuses conducted in one quarter of each subplot (0.025 ha). On six occasions from May 2019 to August 2019, we selected two individuals within or, if absent, closest to the center of each of four, 2-m^2 vegetation sampling areas per subplot. Stems were identified to the species level and their DBH measured using digital calipers. A quarter of the stems sampled for subcanopy DBH were contained within vegetation sampling areas, and all others were sampled outside of designated vegetation sampling areas but within treatment subplots. Mean subplot and species-specific DBH increments were applied to censused stems to infer their growth. Species and site or region-specific allometries [37] were used to calculate subplot aboveground wood biomass.

For seedling and saplings, we censused stems in one randomly selected quarter of each of the 2-m^2 vegetation sampling areas twice: once in June and again in August 2019. We recorded the species, basal diameter and current height, along with the height of each individual at the end of the prior growing season, from branch scars. Following the convention for measuring stems below DBH [40–42], the wood volume of each stem was calculated assuming conical geometry and species-specific wood densities were applied to convert volume to aboveground wood biomass [43].

From aboveground wood biomass increments, we estimated the mean daily $ANPP_w$ (kg C ha^{-1} day^{-1}) of upper canopy trees and annual $ANPP_w$ (kg C ha^{-1} $year^{-1}$) from the cumulative year-long sum of upper canopy, subcanopy, and seedling/sapling aboveground wood production. Daily $ANPP_w$ is upper canopy aboveground wood biomass increment expressed on a daily timestep, scaled to the hectare and multiplied by a site-specific C fraction of 0.48 to convert biomass to C mass [35].

Annual (upper canopy + subcanopy + seedling/sapling) $ANPP_w$ is the November 2018 to November 2019 increment of aboveground wood biomass from all stem size classes scaled to the hectare and converted to C mass. The uncertainty of each $ANPP_w$ estimate was calculated as the standard error of mean (daily or annual) $ANPP_w$ among replicates [35].

In advance of analyzing our results, we examined the sensitivity of our $ANPP_w$ estimates to potential stem swelling above girdled tissues [44], i.e., whether aboveground wood production was inflated because of disproportionately high radial growth at the location of DBH measurements, 30 cm above the removed bark. In early July 2019, on a subset of healthy and girdled trees, we installed a second set of tightly fitted upper dendrometer bands 50 cm above the already installed DBH-positioned bands (n = ≥3 per species). Beginning two weeks after installation, upper and DBH stem diameter increments were recorded concurrently for four weeks from July to August 2019 and again in November 2019. To determine whether disproportionately high radial growth occurred at DBH in girdled trees, we compared the taper of stem diameter increments from upper and lower (DBH positioned) bands in girdled and healthy trees using unpaired t-tests for each species. While moderately significant, *Acer rubrum* was the only species displaying signs of greater taper between the upper and lower growth increments in girdled trees (0.0064 mm day^{-1}) relative to healthy trees (0.0021 mm day^{-1}; $p = 0.06$; data not shown). To test the sensitivity of $ANPP_w$ to a potentially inflated diameter increment in *A. rubrum*, we compared unadjusted and adjusted (i.e., applied a taper adjustment to *A. rubrum*) estimates of aboveground wood production using unpaired t-tests, finding no significant differences between the two approaches (Table A4). Accordingly, our numeric presentation of results and statistical analysis used unadjusted $ANPP_w$ estimates.

2.4. Statistical Analysis

We used a time-series split-plot analysis of variance (ANOVA) model to analyze differences in daily canopy $ANPP_w$ among disturbance severity and disturbance type treatments. Disturbance severity (fully randomized within replicates) was the whole-plot and disturbance type (randomized within each whole-plot) was the split-plot (Table A1). For disturbance treatment comparisons of annual $ANNP_w$, two similar split-split plot models, without time as a factor, were used to analyze differences among disturbance severities, disturbance types, girdled/healthy trees (Table A2) and successional cohort (Table A3) with either girdled/healthy or cohort considered a second (fixed) parameter in the model, respectively. We compared girdled and healthy tree RGR (pooled across disturbance severity and type treatments) and assessed the contribution of each to total annual $ANPP_w$ within disturbance severity and type treatments. Because our girdling treatments and subsequent high frequency (i.e., weekly) stem diameter measurements were concentrated in the upper canopy size class, we limited our analysis of daily $ANPP_w$ and annual $ANPP_w$ by girdled/healthy trees to the upper canopy. We included all canopy strata in the analysis of annual $ANPP_w$ by successional cohort to provide the most comprehensive assessment of successional cohort contributions to annual $ANPP_w$. A priori pairwise comparisons of $ANPP_w$ across time, disturbance severity, disturbance type, successional cohort, and between girdled and healthy trees, were performed using least squares differences (LSD) ($\alpha = 0.05$). Unpaired t-tests were used for pairwise comparisons of girdled and healthy tree annual RGRs among the six most abundant canopy species experiment-wide. Statistical analyses were performed in R (2019) using stats [45] and agricolae [46] statistical analysis packages. Statistical parameters associated with each analysis are presented in Appendix A Tables A1–A3.

Raw data used in this analysis are available via the FoRTE data package [38]: https://github.com/FoRTEXperiment/fortedata. Processed data products and statistical analysis specific to this study are available via: doi: 10.6084/m9.figshare.12442703.

3. Results

3.1. Leaf Area Index

In the first growing season after disturbance, phloem disruption reduced mean end-of-season (Day of Year 213–215) LAI in the 85% disturbance severity treatment by 19% relative to the control and 45% severity treatment (Figure 2A; LSD = 0.62, d.f. = 21, $\alpha = 0.05$). Mean end-of-season LAI was 3.19 in the control plots and the 45%, 2.79 in the 65%, and 2.57 in the 85% disturbance severity treatments, respectively. LAI did not differ significantly between bottom-up and top-down disturbance types (Figure 2B; LSD = 0.49 d.f. = 3, $\alpha = 0.05$).

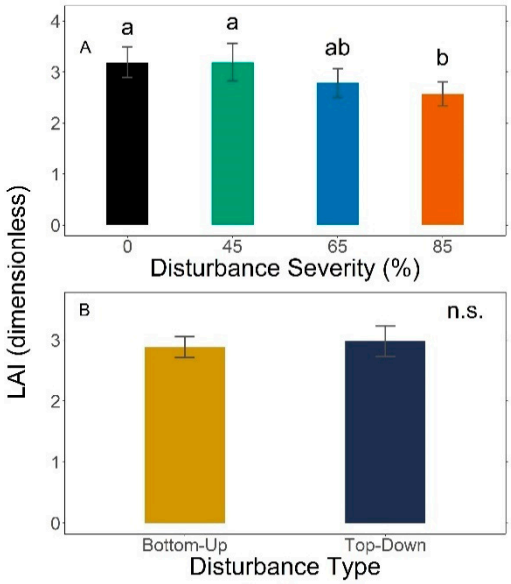

Figure 2. Mean end-of-season (Day of Year 213–215) leaf area index (LAI, ± 1 S.E) by disturbance severity (**A**) and disturbance type (**B**) treatments, three months after phloem-disrupting disturbance. Error bars are the SE of mean leaf area index (LAI) among treatment replicates. Nonoverlapping letters denote significance ($\alpha = 0.05$) among disturbance severity treatments. Significant differences between disturbance types were not detected (n.s.).

3.2. Daily $ANPP_w$ and Disturbance Treatments

At the beginning of June 2019, two weeks after girdling, daily $ANPP_w$ in the control (0% disturbance severity) was significantly greater than that of the 65 and 85% disturbance severities with values of 13.89, 2.99, and 2.98 kg C ha^{-1} day^{-1}, respectively (Figure 3A, LSD = 8.56, d.f. = 336, $\alpha = 0.05$). Within four weeks, however, daily $ANPP_w$ in the 65% disturbance severity reached 37.3 kg C ha^{-1} day^{-1} surpassing that of the control at 24.15 kg C ha^{-1} day^{-1}. After all disturbance severities reached a maximum in mid-July, daily $ANPP_w$ was significantly greater in both the 65 and 85% disturbance severity treatments relative to the control (Figure 3A, LSD = 8.56, d.f. = 336, $\alpha = 0.05$) until values converged again in November 2019. Daily $ANPP_w$ did not differ significantly between top-down and bottom-up disturbance type treatments (Figure 3B, LSD = 5.66, d.f. = 45, $\alpha = 0.05$).

3.3. Relative Growth Rates of Girdled and Healthy Trees

When pooled across treatments to compare the RGRs of girdled and healthy trees, we found species growth responded differently to phloem disruption (Figure 4). Among the six species examined, the RGR of girdled *A. rubrum* (t = 15.3, d.f. = 436, $p < 0.001$), *A. saccharum* (t = 11.29, d.f. = 145, $p < 0.001$), and *P. grandidentata* (t = 18.4, d.f. = 415, $p < 0.001$) were approximately double that of healthy trees of the same species (Figure 4). The RGR of girdled *P. strobus* (t = 2.31, d.f. = 134, $p = 0.02$) was significantly, but more modestly, one-third greater than healthy *P. strobus*. In contrast, *F. grandifolia*

(t = −0.4, d.f. = 345, $p = 0.69$) exhibited no response, while the RGR of girdled *Q. rubra* (t = −17.05, d.f. = 382, $p < 0.001$), a major component of the ecosystem, was two-thirds less than that of healthy *Q. rubra* (Figure 4).

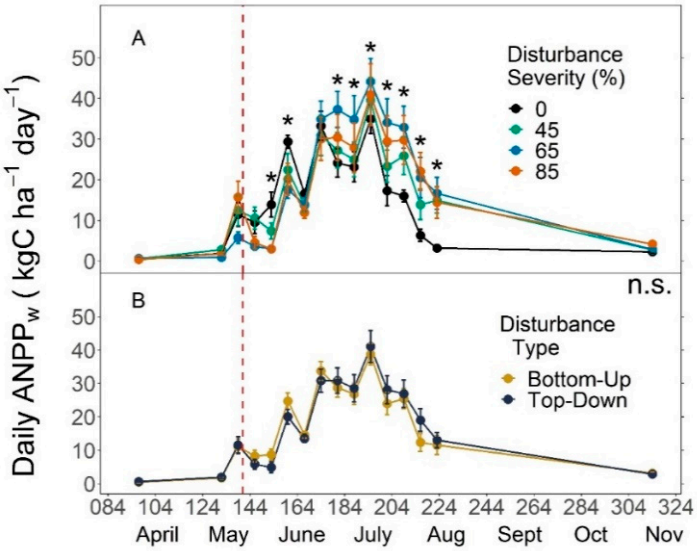

Figure 3. Mean daily upper canopy (>8 cm DBH) aboveground wood net primary production ($ANPP_w$, ± 1 S.E.) by disturbance severity (**A**) and disturbance type (**B**) treatments in the first growing season following phloem-disrupting disturbance (vertical dashed line). Error bars are the SE of mean daily $ANPP_w$ among treatment replicates. Asterisks denote dates on which the control significantly ($\alpha = 0.05$) differed from either the 65 or 85% disturbance severity. Significant differences between disturbance types were not detected (n.s.).

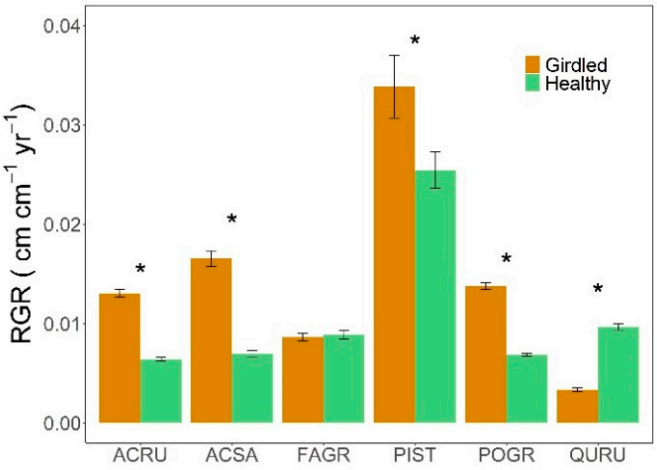

Figure 4. Experiment-wide mean girdled and healthy-tree relative growth rates (RGR, cm cm^{-1} $year^{-1}$) of the six most abundant upper canopy (>8 cm DBH) tree species (Table 1) in the year following phloem-disrupting disturbance. Error bars are the SE of mean relative growth rate (RGR) among girdled or healthy trees of each species. Asterisks denote significance in the pairwise comparison of girdled and healthy trees of each species ($p < 0.05$). Species abbreviations are: *Acer rubrum* (ACRU), *A. saccharum* (ACSA), *Populus grandidentata* (POGR), *Fagus grandifolia* (FAGR), *Pinus strobus* (PIST), *Quercus rubra* (QURU).

3.4. Annual $ANPP_w$ and Disturbance Treatments

The aboveground growth of girdled trees sustained annual $ANPP_w$ in the first growing season after disturbance (Figure 5), resulting in no cumulative treatment effects on year-long production.

Mean annual $ANPP_w$ was 2447 kg C ha^{-1} $year^{-1}$ and did not differ significantly among disturbance severities or between disturbance types (Table A2). The contribution of girdled trees to annual $ANPP_w$ was roughly proportional to the targeted experimental disturbance severity levels, increasing significantly from 47 to 79 and 86% in the 45, 65 and 85% disturbance severity treatments, respectively (Figure 5A; LSD = 576.46, d.f. = 42, $\alpha = 0.05$). Girdled trees in the bottom-up and top-down disturbance treatments accounted for 47% and 64% of annual $ANPP_w$, respectively, with large diameter girdled trees contributing more to annual aboveground wood production in the latter treatment (Figure 5B; LSD = 621.73, d.f. = 3, $\alpha = 0.05$).

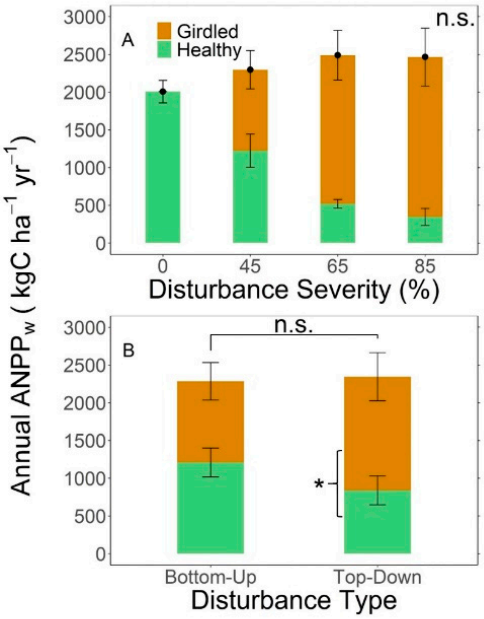

Figure 5. Contributions of girdled and healthy upper canopy (≥8 cm DBH) trees to annual aboveground wood net primary production ($ANPP_w$, ± 1 S.E.) in the control and among disturbance severity (**A**) and disturbance type (**B**) treatments. Healthy and girdled refers to the fraction of $ANPP_w$ supplied by each within a disturbance severity (**A**) and disturbance type (**B**) category. Error bars are the SE of mean annual $ANPP_w$ among treatment replicates. While significant differences were not detected among treatments (n.s), the asterisk denotes that within disturbance types, girdled trees contributed more to $ANPP_w$ in the top-down relative to the bottom-up disturbance treatment (**B**; $\alpha = 0.05$).

Among canopy strata, upper canopy trees were overwhelmingly the primary constituent of annual $ANPP_w$, regardless of disturbance severity and type. Upper canopy trees contributed ~95% of total annual $ANPP_w$ in all disturbance treatments, with subcanopy and seedlings/saplings supplying the remainder of aboveground wood production (Figure A1).

3.5. Successional Cohort Contributions to Annual $ANPP_w$

The contribution of the early successional (*Populus*, *Betula*) species to annual $ANPP_w$ was not significantly different from that of the middle to late successional (*Acer*, *Quercus*, *Pinus*) species among disturbance severities (Figure 6, LSD = 709.07, d.f. = 42, $\alpha = 0.05$). Similarly, the top-down and bottom-up disturbance type treatments did not affect successional cohort contributions to annual $ANPP_w$ (LSD = 743.43, d.f. = 3, $\alpha = 0.05$; data not shown).

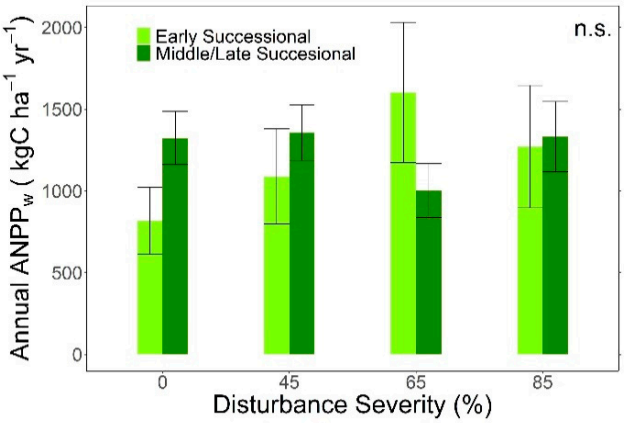

Figure 6. The contribution of early and middle to late successional species cohorts from all canopy strata to annual aboveground wood net primary production (ANPP$_w$, ± 1 S.E.) at each disturbance severity treatment. Error bars are the SE of mean annual ANPP$_w$ among treatment replicates. Significant differences (α = 0.05) between successional cohorts among disturbance severities were not detected (n.s.).

4. Discussion

Contrary to our core hypothesis, the scaled aboveground wood production of girdled trees sustained stand-level ANPP$_w$ in the first year following disturbance, with little to no increase in healthy-tree compensatory growth. Anticipating a reduction during the first growing season in the aboveground wood production of girdled trees, we sampled ANPP$_w$ at a high frequency, expecting healthy tree growth to increase as limiting resource availability increased [24,47–49]. A nearby landscape-scale study, in which a third of all canopy trees were stem girdled, demonstrated that nitrogen and light availability increased within two years after disturbance [24,31], stimulating healthy tree production [26,31]. In our experiment, marginal (<20%) reductions in LAI and the sustained or elevated growth of girdled trees suggest that resource reallocation from girdled to healthy trees was minimal in the first growing season. Consistent with our findings, Flower et al. (2013) found that emerald ash borer infected trees grew for two to five years following initial infestation [47,50], and experimental studies of individual trees report continued but often variable growth along with high survival rates in the first year following stem girdling [13,16,22]. However, we note that the response to phloem disruption varies among disturbance agents and host species, with mortality as rapid as one year following infestation by pine bark beetles [12,25]. In agreement with other studies, we found species' RGRs exhibited different initial responses to girdling [13,18,22], but our analysis demonstrated that these variable growth responses offset one another to stabilize ecosystem production even at the 85% disturbance severity level. Our results extend these findings to the whole ecosystem, demonstrating that the sustained growth of girdled trees was sufficient, despite wide variation among species, to maintain stand-scale ANPP$_w$ across a range of disturbance severities and types for the duration of the first growing season.

The mechanism supporting first-year aboveground wood production in girdled trees is likely sustained C fixation and the retention of photosynthate above the girdle. In healthy trees, recently fixed C is first allocated to the nearest sink before distribution to distal stem and roots sinks [19,51]. When phloem is severed, however, the transport of new photosynthate from the crown to the roots is eliminated entirely and C is retained in aboveground tissues [15]. In our study, higher late-season daily ANPP$_w$ in the middle and high (>65%) disturbance severity treatments suggest a progressive accumulation of C above the girdled phloem in most trees. However, immediate responses to phloem-disruption, as well as the timing of mortality, may vary among species because of differences in plant hormonal patterns [52,53], the depth and extent of tissue damage and repair [23,54] and feedback inhibition of leaf photosynthesis as carbohydrates accumulate [44,55,56]. For example, significantly

lower contributions to $ANPP_W$ from girdled ring-porous *Q. rubra* relative to ring-diffuse *P. grandidentata*, *A. rubrum* and *A. saccharum*, was likely caused by the disruption of the former's more abundant outer tracheid cells [54]. While continued, but temporary, aboveground growth of phloem-disrupted trees is well documented, studies do not agree on how stem girdling alters the partitioning of fixed C among aboveground tissues [13,15,16,57,58]. Further, the impending mortality and growth cessation of phloem-disrupted trees highlights the dynamic nature of C cycling responses to disturbance [59].

With girdled trees continuing to grow regardless of stem size class, top-down and bottom-up disturbance type treatments had no effect on first year $ANPP_W$. As with naturally occurring disturbances, tree size and species identity at our site are intertwined [60] (Figure A2), with larger stems including both early successional *P. grandidentata* and later successional *Q. rubrum*. As a result, disentangling the independent effects of disturbance type from those of species identity is difficult. Our observation that girdled trees contribute more to annual $ANPP_W$ in the top-down rather than bottom-up disturbance (Figure 4) is consistent with observations that larger trees contribute more to stand-scale aboveground production than small trees [47,61–63], a consequence of allometric scaling that occurs in most plants [64]. However, we anticipate differences in $ANPP_W$ to emerge between top-down and bottom-up disturbance treatments in subsequent years as the aboveground wood production of girdled trees declines and, conversely, increases in healthy trees.

Our findings do not support the hypothesis that early successional species contribute more to $ANPP_W$ than later successional species at higher disturbance severities in the first growing season after phloem-disrupting disturbance. At our site, the early successional cohort primarily consists of maturing aspen (*Populus* spp.) that thrive following severe, stand-replacing disturbances such as clear-cut harvesting and fire [65]. Stand-replacing disturbances abruptly increase the quantity of growth-limiting resources including light, nutrients and water, which may favor fast-growing, opportunistic pioneer species that aggressively compete for legacy resources [66–68]. Anticipating a more rapid first-year redistribution of growth-limiting resources from girdled to healthy trees, we expected early successional *Populus* to benefit more than middle and late successional species. Instead, the observed increase in *Populus*'s RGR was similar to that of *Acer* spp. While stable growing season LAI in all but the highest severity disturbance treatment suggests that canopy light distribution changed minimally, increases in nutrient availability may occur more rapidly as leaf and root physiological activity diminishes in parallel with declining nutrient demand from girdled individuals [24,69,70]. Nonetheless, the continued growth of girdled trees suggests physiological decline was nominal and that resource redistribution from girdled to healthy trees, if it occurred, did not stimulate healthy-tree aboveground wood growth in the first year following phloem disruption. As girdled trees die, the canopy deteriorates, and light in the subcanopy becomes more abundant, early successional species may contribute more to aboveground wood production, particularly at high disturbance severities [31].

With little change in LAI during the first growing season following disturbance, we found that subcanopy, seedlings and saplings contributed minimally to $ANPP_W$, even at high disturbance severities. In a nearby study, disturbance-driven changes in LAI were inversely related to subcanopy light availability and growth five years after stem girdling, with the subcanopy constituting nearly half of $ANPP_W$ at severities commensurate with our 65% disturbance severity treatment [31,71]. In comparison, we found that the subcanopy contributed ~5% to annual $ANPP_W$ in the first year following disturbance, an amount comparable to the subcanopy contributions of local undisturbed closed canopy forests [71]. Our observations of limited subcanopy growth are consistent with concurrently measured leaf photosynthesis, chemistry and morphology that suggest no stimulation of subcanopy C fixation in the first growing season [30]. Nonetheless, the subcanopy contribution to total $ANPP_W$ is expected to increase over time as upper canopy LAI declines and subcanopy light availability increases [71–74].

Our finding of sustained $ANPP_W$ in the first growing season following stem girdling signals high initial resistance to disturbance, while highlighting the dynamic and variable nature of C cycling stability. Slowly unfolding disturbances, like phloem-disruption, provide time for the gradual reallocation of

growth-limiting resources in a way that may be less ecologically feasible following more abrupt and severe disturbances. For example, clear-cut harvesting of a nearby forest rapidly increased nitrogen availability [70], but, in the absence of established vegetation, resulted in high leaching [75], which in turn prompted a century-long reduction in net primary production [34]. In contrast, a neighboring stem girdling manipulation displayed high nitrogen retention at disturbance severity levels comparable to our 45% severity treatment [24], sustaining longer term primary production stability [26,31] of this nitrogen-limited ecosystem [75]. Accordingly, initial C cycling responses to disturbance, in turn, may foreshadow longer-term changes in ecosystem function, with immediate responses in ecological processes linked to lasting changes in resource availability [76], microclimate [8] and plant competition [77,78]. While we observed minimal changes in $ANPP_w$ during the first year of our experiment, future stability will likely require the full and efficient transfer of growth-limiting resources to healthy vegetation once girdled trees begin to decline physiologically and their demand for nutrients, water, and light diminishes.

Our results have implications for the management of aboveground wood production following slow-acting disturbances. Because phloem-disrupting disturbances unfold slowly, real-time adaptive forest management strategies may effectively stabilize ecosystem functioning [79,80]. In contrast, adaptive management may be more limited following abrupt disturbances from stand-replacing fire, extreme weather or clear-cut harvesting [81]. In our study, the initial stand-scale stability of $ANPP_w$ suggests that managers have a window in which adaptive strategies could mitigate the long-term effects of slower-acting wood boring pests and pathogens. Such adaptive strategies might include stand-scale, growth-compensating measures such as the seeding or planting of subcanopy vegetation, along with production-efficiency increases associated with amended biodiversity and canopy structure manipulation [80–83]. Studies that document the efficacy of disturbance mitigation strategies are needed to develop broadly effective adaptive management approaches for the array of forest ecosystems and range of disturbance regimes observed in nature [79,84–86].

We note several study limitations. First, allometries for estimating wood biomass were developed from the dimensions and wood densities of healthy trees and their use for girdled trees may introduce error if DBH-aboveground wood biomass relationships change following disturbance. Although plant-scale changes in allometry following phloem disruption have not been reported, an accumulation of C aboveground following phloem disruption is well documented [15,16]. Whether accumulated C is distributed evenly among aboveground structural and nonstructural C pools is unknown and could affect allometries and wood density, respectively [62,87,88]. While tapered swelling within 10 cm of the severed phloem has been reported for some species [21], we found moderately significant radial stem swelling in only one species (*Acer rubrum*) 30 cm above the girdled tissue, where we measured stem diameter. Moreover, while disproportionally high radial growth above the girdle could inflate stand-scaled production, our banding at multiple stem heights revealed the effects of *A. rubrum* swelling on $ANPP_w$ were not statistically significant (Table A4). Even so, allometric equations, when applied outside of their originating ecosystem, site and, in our case, experimental context, will yield estimates with greater unquantifiable uncertainty [89–92].

5. Conclusions

We conclude that a principal mechanism supporting aboveground wood production in the first growing season following a phloem-disrupting disturbance is the sustained growth of girdled trees. While the aboveground growth of *Q. rubra* declined in response to girdling, most species exhibited increased aboveground growth during the first year that, in aggregate, sustained aboveground stand-scale wood production. Counter to our hypothesis, the uninhibited growth of most girdled trees throughout the first growing season following girdling sufficiently sustained stand-scale $ANPP_w$, even in the highest severity treatment affecting ~85% of the woody vegetation. In addition to illuminating high frequency, first-year C cycling responses to phloem disruption, our findings lay the foundation for a comprehensive temporal understanding of the tree-to-ecosystem scale mechanisms

supporting first-year wood production stability [59,93,94]. Finally, our results, when considered in the context of longer-term observations, indicate that the mechanisms supporting C cycling are dynamic, with phloem-disrupted tree growth inevitably giving way to other compensatory processes.

Author Contributions: In preparation of this manuscript, authors contributed the following: writing—original draft preparation, M.S.G.; supervision, C.M.G.; methodology, C.V.; visualization, J.W.A.; conceptualization and writing—review and editing, B.B.-L. All authors have read and agreed to the published version of the manuscript.

Funding: Our work was funded by the National Science Foundation, Division of Environmental Biology, Award 1655095. We thank the University of Michigan Biological Station for logistical and technical support, and the use of research infrastructure.

Conflicts of Interest: The authors declare no conflict of interest, and the funders had no role in the design of the study; in the collection, analyses, or interpretation of data; in the writing of the manuscript, or in the decision to publish the results.

Appendix A

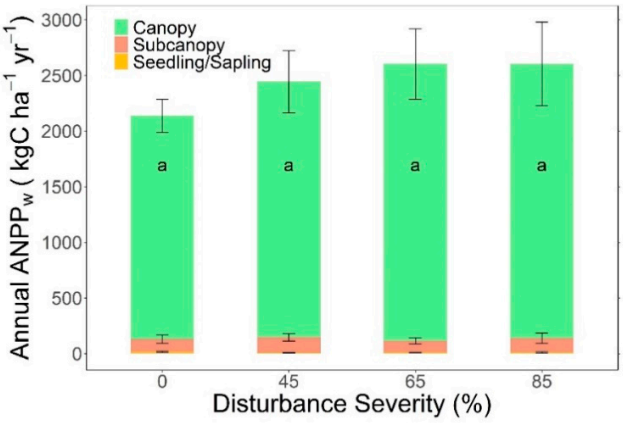

Figure A1. The contributions of upper canopy (≥8 cm diameter breast height, DBH), subcanopy (<8 cm DBH), and seedling/sapling (below DBH height) stems to annual aboveground wood net primary production (ANPP$_w$) (+/− SE) in the first year following disturbance. Error bars are the SE of annual ANPP$_w$ among treatment replicates. Common letters ([a]) signify no significant ($p > 0.05$) difference in total (summed across canopy strata) annual ANPP$_w$ among disturbance severities. ANPP$_w$ ± 1 S.E.

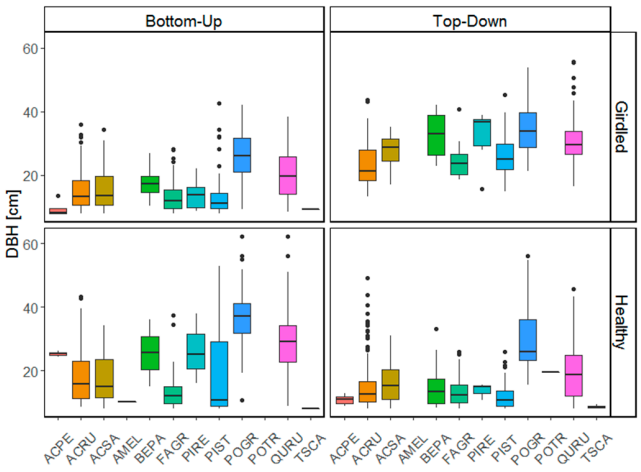

Figure A2. Median (horizontal line), interquartile range (box), 95% confidence intervals (whisker) and outliers (closed circles) of diameter at breast height (DBH) by species for the top-down and bottom-up disturbance type treatments. Species abbreviations are: *Abies Balsamea* (ABBA), *Acer pensylvanicum* (ACPE), *Acer rubrum* (ACRU), *Acer saccharum* (ACSA), *Amelancheir* (AMEL), *Betula papyrifera* (BEPA), *Fagus grandifolia* (FAGR), *Pinus resinosa* (PIRE), *Pinus strobus* (PIST), *Populus grandidentata* (POGR), *Populus tremuloides* (POTR), *Quercus rubra* (QURU), and *Tsuga canadensis* (TSCA).

Table A1. Split-plot time-series analysis of variance (ANOVA) table for daily aboveground wood net primary production ($ANPP_w$), presented in Figure 3 of the manuscript. Week and disturbance type main effects and their interaction were tested against more conservative error terms to account for restricted randomization, whereas the main effect disturbance severity and its interaction with week were tested against the residual error. Asterisks indicate an interaction between two or more parameters.

Source	DF	Type I SS	MS	F Ratio	*p* Value
Replicate	3	4124	1375	6.501	0.001
Week	15	70,168	4678	22.126	<0.001
Error 1 (rep*week)	45	9514	211		
Disturbance Type	1	17	17	0.017	0.904
Error 2 (rep*type)	3	2951	984		
Week*Type	15	1035	69	1.091	0.391
Error 3 (rep*week*type)	45	2846	63		
Disturbance Severity	3	962	321	4.235	0.006
Week*Severity	45	7706	171	2.261	<0.001
Residual Error	336	25,442	76		

Table A2. Split-plot analysis of variance (ANOVA) table for annual upper canopy (DBH ≥ 8 cm) aboveground wood net primary production ($ANPP_w$) presented in Figure 4 of the manuscript. Disturbance type and treatment (girdled/not-girdled) main effects and their interaction terms were tested against more conservative error terms to account for restricted randomization, whereas the main effect disturbance severity and its interaction with treatment were tested against the residual error. Asterisks indicate an interaction between two or more parameters.

Source	DF	Type I SS	MS	F Ratio	*p* Value
Replicate	3	2,007,145	669,048	1.114	0.466
Disturbance Type	1	14,387	14,387	0.024	0.887
Error 1 (rep*type)	3	1,800,940	600,313		
Treatment	1	1,139,523	1,139,523	2.053	0.247
Error 2 (rep*treatment)	3	1,665,033	555,011		
Treatment*Disturbance Type	1	2,560,243	2,560,243	8.385	0.063
Error 3 (rep*treatment*type)	3	915,984	305,328		
Disturbance Severity	3	591,929	197,310	0.605	0.616
Disturbance Severity*Treatment	3	36,073,959	12,024,653	36.843	<0.001
Residual Error	42	13,707,781	326,376		

Table A3. Split-plot analysis of variance (ANOVA) table for annual aboveground wood net primary production ($ANPP_w$), presented in Figure 5 of the manuscript. Disturbance type and successional cohort (cohort) main effects and their interaction were tested against more conservative error terms to account for restricted randomization, whereas the main effect disturbance severity and its interaction with cohort were tested against the residual error. Asterisks indicate an interaction between two or more parameters.

Source	DF	Type I SS	MS	F Ratio	*p* Value
Replicate	3	2,548,508	849,503	1.261	0.427
Disturbance Type	1	18,509	18,509	0.027	0.879
Error 1 (rep*type)	3	2,020,717	673,572		
Cohort	1	56,444	56,444	0.035	0.863
Error 2 (rep*cohort)	3	4,832,009	1,610,670		
Cohort*Disturbance Type	1	934,523	934,523	2.141	0.240
Error 3 (rep*cohort*type)	3	1,309,686	436,562		
Disturbance Severity	3	577,586	192,529	0.390	0.761
Disturbance Severity*Cohort	3	2,710,208	903,403	1.829	0.156
Residual Error	42	20,740,309	493,817		

Table A4. Annual upper canopy (DBH ≥ 8 cm) aboveground wood net primary production ($ANPP_w$) values unadjusted for swelling and adjusted for *Acer rubrum* DBH swelling (30 cm) above girdled tissue. Dendrometer bands (N = ≥3 per species) were fitted to stems at two heights 50 cm apart and their diameter increments recorded concurrently on five occasions between July 2019 and November 2019. Among the five species examined, only *Acer rubrum* exhibited significantly greater diameter growth taper in girdled trees ($p = 0.06$). To evaluate the sensitivity of annual $ANPP_w$ to *Acer rubrum* swelling, we scaled production separately including (unadjusted) and excluding (adjusted) *Acer rubrum* contributions to annual $ANPP_w$. We found no significant differences between unadjusted and adjusted annual $ANPP_w$ estimates (unpaired *t*-tests; $\alpha = 0.05$), nor did the unadjusted or adjusted $ANPP_w$ estimates affect the outcome of pairwise treatment comparisons (least squares differences, pairwise comparisons; $\alpha = 0.1$). Common superscripted letters ([a]) among treatments indicate no significant pairwise differences when unadjusted or adjusted annual $ANPP_w$ values were used in analyses. $ANPP_w$ ± 1 S.E.

	Annual Canopy $ANPP_w$		
Severity (%)	Unadjusted	Adjusted	*p* value
Control	2007 (148) [a]	2007 (148) [a]	-
45	2297 (280) [a]	2208 (268) [a]	0.821
65	2489 (317) [a]	2309 (332) [a]	0.701
85	2465 (376) [a]	2209 (381) [a]	0.639
Disturbance Type			
Bottom-Up	2285 (182) [a]	2080 (192) [a]	0.446
Top-Down	2344 (226) [a]	2286 (212) [a]	0.852

References

1. Hicke, J.A.; Allen, C.D.; Desai, A.R.; Dietze, M.C.; Hall, R.J.; Ted Hogg, E.H.; Kashian, D.M.; Moore, D.; Raffa, K.F.; Sturrock, R.N.; et al. Effects of Biotic Disturbances on Forest Carbon Cycling in the United States and Canada. *Glob. Chang. Biol.* **2012**, *18*, 7–34. [CrossRef]
2. Kautz, M.; Anthoni, P.; Meddens, A.J.H.; Pugh, T.A.M.; Arneth, A. Simulating the Recent Impacts of Multiple Biotic Disturbances on Forest Carbon Cycling across the United States. *Glob. Chang. Biol.* **2018**, *24*, 2079–2092. [CrossRef] [PubMed]
3. Flower, C.E.; Gonzalez-Meler, M.A. Responses of Temperate Forest Productivity to Insect and Pathogen Disturbances. *Annu. Rev. Plant Biol.* **2015**, *66*, 547–569. [CrossRef] [PubMed]
4. Hancock, J.E.; Arthur, M.A.; Weathers, K.C.; Lovett, G.M. Carbon Cycling along a Gradient of Beech Bark Disease Impact in the Catskill Mountains, New York. *Can. J. For. Res.* **2008**, *38*, 1267–1274. [CrossRef]
5. Kautz, M.; Meddens, A.J.H.; Hall, R.J.; Arneth, A. Biotic Disturbances in Northern Hemisphere Forests—A Synthesis of Recent Data, Uncertainties and Implications for Forest Monitoring and Modelling. *Glob. Ecol. Biogeogr.* **2017**, *26*, 533–552. [CrossRef]
6. Atkins, J.W.; Bond-Lamberty, B.; Fahey, R.T.; Hardiman, B.S.; Haber, L.; Stuart-Haëntjens, E.; LaRue, E.; McNeil, B.; Orwig, D.A.; Stovall, A.E.S.; et al. Multidimensional Structural Characterization Is Required to Detect and Differentiate Among Moderate Disturbance Agents. *Preprints* **2019**. [CrossRef]
7. Elkinton, J.S.; Liebhold, A.M. Population Dynamics of Gypsy Moth in North America. *Annu. Rev. Entomol.* **1990**, *35*, 571–596. [CrossRef]
8. Lovett, G.M.; Canham, C.D.; Arthur, M.A.; Weathers, K.C.; Fitzhugh, R.D. Forest Ecosystem Responses to Exotic Pests and Pathogens in Eastern North America. *BioScience* **2006**, *56*, 395–405. [CrossRef]
9. Peltzer, D.A.; Allen, R.B.; Lovett, G.M.; Whitehead, D.; Wardle, D.A. Effects of Biological Invasions on Forest Carbon Sequestration. *Glob. Chang. Biol.* **2010**, *16*, 732–746. [CrossRef]
10. Krasny, M.E.; Whitmore, M.C. Gradual and Sudden Forest Canopy Gaps in Allegheny Northern Hardwood Forests. *Can. J. For. Res.* **1992**, *22*, 139–143. [CrossRef]
11. Reyes, G.P.; Kneeshaw, D. Moderate-Severity Disturbance Dynamics in Abies Balsamea-Betula Spp. Forests: The Relative Importance of Disturbance Type and Local Stand and Site Characteristics on Woody Vegetation Response. *Écoscience* **2008**, *15*, 241–249. [CrossRef]

12. Hubbard, R.M.; Rhoades, C.C.; Elder, K.; Negron, J. Changes in Transpiration and Foliage Growth in Lodgepole Pine Trees Following Mountain Pine Beetle Attack and Mechanical Girdling. *For. Ecol. Manag.* **2013**, *289*, 312–317. [CrossRef]
13. Mei, L.; Xiong, Y.; Gu, J.; Wang, Z.; Guo, D. Whole-Tree Dynamics of Non-Structural Carbohydrate and Nitrogen Pools across Different Seasons and in Response to Girdling in Two Temperate Trees. *Oecologia* **2015**, *177*, 333–344. [CrossRef] [PubMed]
14. Murakami, P.F.; Schaberg, P.G.; Shane, J.B. Stem Girdling Manipulates Leaf Sugar Concentrations and Anthocyanin Expression in Sugar Maple Trees during Autumn. *Tree Physiol.* **2008**, *28*, 1467–1473. [CrossRef] [PubMed]
15. Winkler, A.; Oberhuber, W. Cambial Response of Norway Spruce to Modified Carbon Availability by Phloem Girdling. *Tree Physiol.* **2017**, *37*, 1527–1535. [CrossRef] [PubMed]
16. Fajstavr, M.; Giagli, K.; Vavrčík, H.; Gryc, V.; Urban, J. The Effect of Stem Girdling on Xylem and Phloem Formation in Scots Pine. *Silva Fenn.* **2017**, *51*. [CrossRef]
17. Maier, C.A.; Johnsen, K.H.; Clinton, B.D.; Ludovici, K.H. Relationships between Stem CO2 Efflux, Substrate Supply, and Growth in Young Loblolly Pine Trees. *New Phytol.* **2010**, *185*, 502–513. [CrossRef]
18. López, R.; Brossa, R.; Gil, L.; Pita, P. Stem Girdling Evidences a Trade-off between Cambial Activity and Sprouting and Dramatically Reduces Plant Transpiration Due to Feedback Inhibition of Photosynthesis and Hormone Signaling. *Front. Plant Sci.* **2015**, *6*. [CrossRef]
19. Jordan, M.-O.; Habib, R. Mobilizable Carbon Reserves in Young Peach Trees as Evidenced by Trunk Girdling Experiments. *J. Exp. Bot.* **1996**, *47*, 79–87. [CrossRef]
20. Dunn, J.P.; Lorio, P.L. Effects of Bark Girdling on Carbohydrate Supply and Resistance of Loblolly Pine to Southern Pine Beetle (Dendroctonus Frontalis Zimm.) Attack. *For. Ecol. Manag.* **1992**, *50*, 317–330. [CrossRef]
21. De Schepper, V.; Steppe, K.; Van Labeke, M.-C.; Lemeur, R. Detailed Analysis of Double Girdling Effects on Stem Diameter Variations and Sap Flow in Young Oak Trees. *Environ. Exp. Bot.* **2010**, *68*, 149–156. [CrossRef]
22. Regier, N.; Streb, S.; Zeeman, S.C.; Frey, B. Seasonal Changes in Starch and Sugar Content of Poplar (Populus Deltoides × Nigra Cv. Dorskamp) and the Impact of Stem Girdling on Carbohydrate Allocation to Roots. *Tree Physiol.* **2010**, *30*, 979–987. [CrossRef] [PubMed]
23. Rademacher, T.T.; Basler, D.; Eckes-Shephard, A.H.; Fonti, P.; Friend, A.D.; Le Moine, J.; Richardson, A.D. Using Direct Phloem Transport Manipulation to Advance Understanding of Carbon Dynamics in Forest Trees. *Front. Glob. Chang.* **2019**, *2*. [CrossRef]
24. Nave, L.E.; Gough, C.M.; Maurer, K.D.; Bohrer, G.; Hardiman, B.S.; Moine, J.L.; Munoz, A.B.; Nadelhoffer, K.J.; Sparks, J.P.; Strahm, B.D.; et al. Disturbance and the Resilience of Coupled Carbon and Nitrogen Cycling in a North Temperate Forest. *J. Geophys. Res. Biogeosci.* **2011**, *116*. [CrossRef]
25. Edburg, S.L.; Hicke, J.A.; Brooks, P.D.; Pendall, E.G.; Ewers, B.E.; Norton, U.; Gochis, D.; Gutmann, E.D.; Meddens, A.J. Cascading Impacts of Bark Beetle-Caused Tree Mortality on Coupled Biogeophysical and Biogeochemical Processes. *Front. Ecol. Environ.* **2012**, *10*, 416–424. [CrossRef]
26. Gough, C.M.; Hardiman, B.S.; Nave, L.E.; Bohrer, G.; Maurer, K.D.; Vogel, C.S.; Nadelhoffer, K.J.; Curtis, P.S. Sustained Carbon Uptake and Storage Following Moderate Disturbance in a Great Lakes Forest. *Ecol. Appl.* **2013**, *23*, 1202–1215. [CrossRef]
27. Dietze, M.C.; Matthes, J.H. A General Ecophysiological Framework for Modelling the Impact of Pests and Pathogens on Forest Ecosystems. *Ecol. Lett.* **2014**, *17*, 1418–1426. [CrossRef]
28. Amiro, B.D.; Barr, A.G.; Barr, J.G.; Black, T.A.; Bracho, R.; Brown, M.; Chen, J.; Clark, K.L.; Davis, K.J.; Desai, A.R.; et al. Ecosystem Carbon Dioxide Fluxes after Disturbance in Forests of North America. *J. Geophys. Res. Biogeosci.* **2010**, *115*. [CrossRef]
29. Högberg, P.; Nordgren, A.; Buchmann, N.; Taylor, A.F.S.; Ekblad, A.; Högberg, M.N.; Nyberg, G.; Ottosson-Löfvenius, M.; Read, D.J. Large-Scale Forest Girdling Shows That Current Photosynthesis Drives Soil Respiration. *Nature* **2001**, *411*, 789–792. [CrossRef]
30. Gough, C.M.; Atkins, J.W.; Bond-Lamberty, B.; Agee, E.A.; Dorheim, K.R.; Fahey, R.T.; Grigri, M.S.; Haber, L.T.; Mathes, K.C.; Pennington, S.C.; et al. Forest Structural Complexity and Biomass Predict First-Year Carbon Cycling Responses to Disturbance. *Ecosystems* **2020**. [CrossRef]
31. Stuart-Haëntjens, E.J.; Curtis, P.S.; Fahey, R.T.; Vogel, C.S.; Gough, C.M. Net Primary Production of a Temperate Deciduous Forest Exhibits a Threshold Response to Increasing Disturbance Severity. *Ecology* **2015**, *96*, 2478–2487. [CrossRef] [PubMed]

32. Parrish, J.A.D.; Bazzaz, F.A. Responses of Plants from Three Successional Communities to a Nutrient Gradient. *J. Ecol.* **1982**, *70*, 233–248. [CrossRef]
33. NOAA National Centers for Environmental Information, Climate at a Glance: County Time Series. Available online: https://www.ncdc.noaa.gov/cag/ (accessed on 24 November 2020).
34. Gough, C.M.; Vogel, C.S.; Harrold, K.H.; George, K.; Curtis, P.S. The Legacy of Harvest and Fire on Ecosystem Carbon Storage in a North Temperate Forest. *Glob. Chang. Biol.* **2007**, *13*, 1935–1949. [CrossRef]
35. Gough, C.M.; Vogel, C.S.; Schmid, H.P.; Su, H.-B.; Curtis, P.S. Multi-Year Convergence of Biometric and Meteorological Estimates of Forest Carbon Storage. *Agric. For. Meteorol.* **2008**, *148*, 158–170. [CrossRef]
36. Pearsall, D.R. Landscape Ecosystems of the University of Michigan Biological Station: Ecosystem Diversity and Ground-Cover Diversity. Ph.D. Thesis, University of Michigan, Ann Arbor, MI, USA, 1995.
37. Cooper, A.W. Above-Ground Biomass Accumulation and Net Primary Production During the First 70 Years of Succession in Populus Grandidentata Stands on Poor Sites in Northern Lower Michigan. In *Forest Succession: Concepts and Application*; West, D.C., Shugart, H.H., Botkin, D.B., Eds.; Springer Advanced Texts in Life Sciences; Springer: New York, NY, USA, 1981; pp. 339–360. [CrossRef]
38. Atkins, J.W.; Agee, E.; Barry, A.; Dahlin, K.M.; Dorheim, K.; Grigri, M.S.; Haber, L.T.; Hickey, L.J.; Kamoske, A.G.; Mathes, K.; et al. The *Fortedata* R Package: Open-Science Datasets from a Manipulative Experiment Testing Forest Resilience. *Earth Syst. Sci. Data Discuss.* **2020**, 1–18. [CrossRef]
39. Gough, C.M.; Flower, C.E.; Vogel, C.S.; Dragoni, D.; Curtis, P.S. Whole-Ecosystem Labile Carbon Production in a North Temperate Deciduous Forest. *Agric. For. Meteorol.* **2009**, *149*, 1531–1540. [CrossRef]
40. Woodall, C.W.; Heath, L.S.; Domke, G.M.; Nichols, M.C. Methods and Equations for Estimating Aboveground Volume, Biomass, and Carbon for Trees in the U.S. Forest Inventory 2010. *Gen. Tech. Rep.* **2011**. [CrossRef]
41. Smith, J.E.; Heath, L.S.; Jenkins, J.C. *Forest Volume-to-Biomass Models and Estimates of Mass for Live and Standing Dead Trees of U.S. Forests*; US Department of Agriculture, Forest Service, Northeastern Research Station: Newtown Square, PA, USA, 2003; Volume 298. [CrossRef]
42. Olschofsky, K.; Mues, V.; Köhl, M. Operational Assessment of Aboveground Tree Volume and Biomass by Terrestrial Laser Scanning. *Comput. Electron. Agric.* **2016**, *127*, 699–707. [CrossRef]
43. Chave, J.; Coomes, D.; Jansen, S.; Lewis, S.L.; Swenson, N.G.; Zanne, A.E. Towards a Worldwide Wood Economics Spectrum. *Ecol. Lett.* **2009**, *12*, 351–366. [CrossRef]
44. De Schepper, V.; Vanhaecke, L.; Steppe, K. Localized Stem Chilling Alters Carbon Processes in the Adjacent Stem and in Source Leaves. *Tree Physiol.* **2011**, *31*, 1194–1203. [CrossRef]
45. R Core Team. R: A Language and Evironment for Statistical Coputing. Foundation for Statistical Computing 2019. Available online: https://www.r-project.org/ (accessed on 01 August 2019).
46. De Mendiburu, F. Agricolae: Statistical Procedures for Agricultural Research. *R Package Version 1.3-3*. 2020. Available online: https://cran.r-project.org/package=agricolae (accessed on 02 January 2020).
47. Flower, C.E.; Knight, K.S.; Gonzalez-Meler, M.A. Impacts of the Emerald Ash Borer (Agrilus Planipennis Fairmaire) Induced Ash (Fraxinus Spp.) Mortality on Forest Carbon Cycling and Successional Dynamics in the Eastern United States. *Biol. Invasions* **2013**, *15*, 931–944. [CrossRef]
48. Lewis, K.J.; Thompson, R.D.; Trummer, L. Growth Response of Spruce Infected by Inonotus Tomentosus in Alaska and Interactions with Spruce Beetle. *Can. J. For. Res.* **2005**, *35*, 1455–1463. [CrossRef]
49. Veblen, T.T.; Hadley, K.S.; Reid, M.S.; Rebertus, A.J. The Response of Subalpine Forests to Spruce Beetle Outbreak in Colorado. *Ecology* **1991**, *72*, 213–231. [CrossRef]
50. Knight, K.S.; Brown, J.P.; Long, R.P. Factors Affecting the Survival of Ash (Fraxinus Spp.) Trees Infested by Emerald Ash Borer (Agrilus Planipennis). *Biol. Invasions* **2013**, *15*, 371–383. [CrossRef]
51. Kozlowski, T.T. Carbohydrate Sources and Sinks in Woody Plants. *Bot. Rev.* **1992**, *58*, 107–222. [CrossRef]
52. Asao, S.; Ryan, M.G. Carbohydrate Regulation of Photosynthesis and Respiration from Branch Girdling in Four Species of Wet Tropical Rain Forest Trees. *Tree Physiol.* **2015**, *35*, 608–620. [CrossRef] [PubMed]
53. Domec, J.-C.; Pruyn, M.L. Bole Girdling Affects Metabolic Properties and Root, Trunk and Branch Hydraulics of Young Ponderosa Pine Trees. *Tree Physiol.* **2008**, *28*, 1493–1504. [CrossRef]
54. Noel, A.R.A. The Girdled Tree. *Bot. Rev.* **1970**, *36*, 162–195. [CrossRef]
55. De Schepper, V.; Steppe, K. Tree Girdling Responses Simulated by a Water and Carbon Transport Model. *Ann. Bot.* **2011**, *108*, 1147–1154. [CrossRef]
56. Myers, D.A.; Thomas, R.B.; DeLucia, E.H. Photosynthetic Responses of Loblolly Pine (Pinus Taeda) Needles to Experimental Reduction in Sink Demand. *Tree Physiol.* **1999**, *19*, 235–242. [CrossRef]

57. Wilson, B.F.; Gartner, B.L. Effects of Phloem Girdling in Conifers on Apical Control of Branches, Growth Allocation and Air in Wood. *Tree Physiol.* **2002**, *22*, 347–353. [CrossRef] [PubMed]
58. Vemmos, S.N.; Papagiannopoulou, A.; Coward, S. Effects of Shoot Girdling on Photosynthetic Capacity, Leaf Carbohydrate, and Bud Abscission in Pistachio (*Pistacia Vera* L.). *Photosynthetica* **2012**, *50*, 35–48. [CrossRef]
59. Hillebrand, H.; Langenheder, S.; Lebret, K.; Lindström, E.; Östman, Ö.; Striebel, M. Decomposing Multiple Dimensions of Stability in Global Change Experiments. *Ecol. Lett.* **2018**, *21*, 21–30. [CrossRef] [PubMed]
60. Gough, C.M.; Vogel, C.S.; Hardiman, B.; Curtis, P.S. Wood Net Primary Production Resilience in an Unmanaged Forest Transitioning from Early to Middle Succession. *For. Ecol. Manag.* **2010**, *260*, 36–41. [CrossRef]
61. Bruhn, D.; Leverenz, J.W.; Saxe, H. Effects of Tree Size and Temperature on Relative Growth Rate and Its Components of Fagus Sylvatica Seedlings Exposed to Two Partial Pressures of Atmospheric [CO_2]. *New Phytol.* **2000**, *146*, 415–425. [CrossRef]
62. Poorter, H.; Niklas, K.J.; Reich, P.B.; Oleksyn, J.; Poot, P.; Mommer, L. Biomass Allocation to Leaves, Stems and Roots: Meta-Analyses of Interspecific Variation and Environmental Control. *New Phytol.* **2012**, *193*, 30–50. [CrossRef] [PubMed]
63. Mensah, S.; Kakaï, R.G.; Seifert, T. Patterns of Biomass Allocation between Foliage and Woody Structure: The Effects of Tree Size and Specific Functional Traits. *Ann. For. Res.* **2016**, *59*, 49–60. [CrossRef]
64. Niklas, K.J. *Plant Allometry: The Scaling of Form and Process*; University of Chicago Press: Chicago, IL, USA, 1994.
65. Caspersen, J.P.; Pacala, S.W. Successional Diversity and Forest Ecosystem Function. *Ecol. Res.* **2001**, *16*, 895–903. [CrossRef]
66. Bormann, F.H.; Likens, G.E. Catastrophic Disturbance and the Steady State in Northern Hardwood Forests: A New Look at the Role of Disturbance in the Development of Forest Ecosystems Suggests Important Implications for Land-Use Policies. *Am. Sci.* **1979**, *67*, 660–669.
67. Curtis, P.S.; Vogel, C.S.; Wang, X.; Pregitzer, K.S.; Zak, D.R.; Lussenhop, J.; Kubiske, M.; Teeri, J.A. Gas Exchange, Leaf Nitrogen, and Growth Efficiency of Populus Tremuloides in a Co2-Enriched Atmosphere. *Ecol. Appl.* **2000**, *10*, 3–17. [CrossRef]
68. Foster, D.R.; Aber, J.D.; Melillo, J.M.; Bowden, R.D.; Bazzaz, F.A. Forest Response to Disturbance and Anthropogenic Stress. *BioScience* **1997**, *47*, 437–445. [CrossRef]
69. Edwards, N.T.; Ross-Todd, B.M. The Effects of Stem Girdling on Biogeochemical Cycles within a Mixed Deciduous Forest in Eastern Tennessee. I. Soil Solution Chemistry, Soil Respiration, Litterfall and Root Biomass Studies. *Oecologia* **1979**, *40*, 247–257. [CrossRef] [PubMed]
70. White, L.L.; Zak, D.R.; Barnes, B.V. Biomass Accumulation and Soil Nitrogen Availability in an 87-Year-Old Populus Grandidentata Chronosequence. *For. Ecol. Manag.* **2004**, *191*, 121–127. [CrossRef]
71. Fahey, R.T.; Stuart-Haëntjens, E.J.; Gough, C.M.; De La Cruz, A.; Stockton, E.; Vogel, C.S.; Curtis, P.S. Evaluating Forest Subcanopy Response to Moderate Severity Disturbance and Contribution to Ecosystem-Level Productivity and Resilience. *For. Ecol. Manag.* **2016**, *376*, 135–147. [CrossRef]
72. Canham, C.D. Growth and Canopy Architecture of Shade-Tolerant Trees: Response to Canopy Gaps. *Ecology* **1988**, *69*, 786–795. [CrossRef]
73. Kaelke, C.M.; Kruger, E.L.; Reich, P.B. Trade-Offs in Seedling Survival, Growth, and Physiology among Hardwood Species of Contrasting Successional Status along a Light-Availability Gradient. *Can. J. For. Res.* **2001**, *31*, 1602–1616. [CrossRef]
74. Dyer, J.H.; Gower, S.T.; Forrester, J.A.; Lorimer, C.G.; Mladenoff, D.J.; Burton, J.I. Effects of Selective Tree Harvests on Aboveground Biomass and Net Primary Productivity of a Second-Growth Northern Hardwood Forest. *Can. J. For. Res.* **2010**, *40*, 2360–2369. [CrossRef]
75. Nave, L.E.; Vance, E.D.; Swanston, C.W.; Curtis, P.S. Impacts of Elevated N Inputs on North Temperate Forest Soil C Storage, C/N, and Net N-Mineralization. *Geoderma* **2009**, *153*, 231–240. [CrossRef]
76. Jenkins, J.C.; Aber, J.D.; Canham, C.D. Hemlock Woolly Adelgid Impacts on Community Structure and N Cycling Rates in Eastern Hemlock Forests. *Can. J. For. Res.* **1999**, *29*, 630–645. [CrossRef]
77. Yorks, T.E.; Leopold, D.J.; Raynal, D.J. Effects of Tsuga Canadensis Mortality on Soil Water Chemistry and Understory Vegetation: Possible Consequences of an Invasive Insect Herbivore. *Can. J. For. Res.* **2003**, *33*, 1525–1537. [CrossRef]

78. Jenkins, J.C.; Canham, C.D.; Barten, P.K. Predicting Long-Term Forest Development Following Hemlock Mortality. In Proceedings of the Symposium on Sustainable Management of Hemlock Ecosystems in Eastern North America, Durham, NH, USA, 22–24 June 1999; McManus, K.A., Shields, K.S., Souto, D.R., Eds.; NRC Research Press: Ottowa, QC, Canada, 2000; Volume 267.
79. Thom, D.; Golivets, M.; Edling, L.; Meigs, G.W.; Gourevitch, J.D.; Sonter, L.J.; Galford, G.L.; Keeton, W.S. The Climate Sensitivity of Carbon, Timber, and Species Richness Covaries with Forest Age in Boreal–Temperate North America. *Glob. Chang. Biol.* **2019**, *25*, 2446–2458. [CrossRef] [PubMed]
80. Buma, B.; Wessman, C.A. Forest Resilience, Climate Change, and Opportunities for Adaptation: A Specific Case of a General Problem. *For. Ecol. Manag.* **2013**, *306*, 216–225. [CrossRef]
81. Harris, R.M.B.; Beaumont, L.J.; Vance, T.R.; Tozer, C.R.; Remenyi, T.A.; Perkins-Kirkpatrick, S.E.; Mitchell, P.J.; Nicotra, A.B.; McGregor, S.; Andrew, N.R.; et al. Biological Responses to the Press and Pulse of Climate Trends and Extreme Events. *Nat. Clim. Chang.* **2018**, *8*, 579–587. [CrossRef]
82. Bradford, J.B.; D'Amato, A.W. Recognizing Trade-Offs in Multi-Objective Land Management. *Front. Ecol. Environ.* **2012**, *10*, 210–216. [CrossRef]
83. Creutzburg, M.K.; Scheller, R.M.; Lucash, M.S.; LeDuc, S.D.; Johnson, M.G. Forest Management Scenarios in a Changing Climate: Trade-Offs between Carbon, Timber, and Old Forest. *Ecol. Appl.* **2017**, *27*, 503–518. [CrossRef]
84. Birdsey, R.; Pregitzer, K.; Lucier, A. Forest Carbon Management in the United States. *J. Environ. Qual.* **2006**, *35*, 1461–1469. [CrossRef]
85. Williams, C.A.; Collatz, G.J.; Masek, J.; Goward, S.N. Carbon Consequences of Forest Disturbance and Recovery across the Conterminous United States: Forest Disturbance and Carbon Dynamics. *Glob. Biogeochem. Cycles* **2012**, *26*. [CrossRef]
86. Albrich, K.; Rammer, W.; Thom, D.; Seidl, R. Trade-Offs between Temporal Stability and Level of Forest Ecosystem Services Provisioning under Climate Change. *Ecol. Appl.* **2018**, *28*, 1884–1896. [CrossRef]
87. Würth, M.K.R.; Peláez-Riedl, S.; Wright, S.J.; Körner, C. Non-Structural Carbohydrate Pools in a Tropical Forest. *Oecologia* **2005**, *143*, 11–24. [CrossRef]
88. Zheng, Z.; Feng, Z.; Cao, M.; Li, Z.; Zhang, J. Forest Structure and Biomass of a Tropical Seasonal Rain Forest in Xishuangbanna, Southwest China1. *Biotropica* **2006**, *38*, 318–327. [CrossRef]
89. Clark, D.A.; Brown, S.; Kicklighter, D.W.; Chambers, J.Q.; Thomlinson, J.R.; Ni, J. Measuring Net Primary Production in Forests: Concepts and Field Methods. *Ecol. Appl.* **2001**, *11*, 356–370. [CrossRef]
90. Dietze, M.C.; Wolosin, M.S.; Clark, J.S. Capturing Diversity and Interspecific Variability in Allometries: A Hierarchical Approach. *For. Ecol. Manag.* **2008**, *256*, 1939–1948. [CrossRef]
91. Fatemi, F.R.; Yanai, R.D.; Hamburg, S.P.; Vadeboncoeur, M.A.; Arthur, M.A.; Briggs, R.D.; Levine, C.R. Allometric Equations for Young Northern Hardwoods: The Importance of Age-Specific Equations for Estimating Aboveground Biomass. *Can. J. For. Res.* **2011**, *41*, 881–891. [CrossRef]
92. Yanai, R.D.; Battles, J.J.; Richardson, A.D.; Blodgett, C.A.; Wood, D.M.; Rastetter, E.B. Estimating Uncertainty in Ecosystem Budget Calculations. *Ecosystems* **2010**, *13*, 239–248. [CrossRef]
93. Blanco, J.A.; Seely, B.; Welham, C.; Kimmins, J.P.; Seebacher, T.M. Testing the Performance of a Forest Ecosystem Model (FORECAST) against 29 Years of Field Data in a Pseudotsuga Menziesii Plantation. *Can. J. For. Res.* **2007**, *37*, 1808–1820. [CrossRef]
94. Weng, E.; Luo, Y. Relative Information Contributions of Model vs. Data to Short- and Long-Term Forecasts of Forest Carbon Dynamics. *Ecol. Appl.* **2011**, *21*, 1490–1505. [CrossRef] [PubMed]